1. General

AerMet 100, a further development of AF 1410 (Chapter 1224), is currently being used in landing gear applications. Because of its high strength, hardness, and fracture toughness, it has potential applications in many critical components in aerospace structures. The AF 1410 alloy has MIL-HDBK 5G (Ref. 1) S-Basis design values of F_{tu} = 235 ksi and F_{ty} = 215 ksi; the corresponding values for AerMet 100 are F_{tu} = 280 ksi and F_{ty} = 235 ksi for the 900F aged condition. Typical K_{Ic} values for AF 1410 vary from 130 to 150 ksi$\sqrt{in}$. with the lower values characteristic of the SL crack orientation in plate; corresponding K_{Ic} values for AerMet 100 forgings (aged at 900F) vary from 105 to 125 ksi$\sqrt{in}$. Aging AerMet 100 at 875F increases the tensile and yield strengths by about 10 ksi with typical K_{Ic} values from 80 to 100 ksi$\sqrt{in}$. These improved strength properties of AerMet 100 coupled with high fracture toughness were obtained by increases in the content of C, Ni, and Cr and reduction in the amount of tramp elements by careful raw material selection and control of the melting practice. From the available information, AerMet 100, on balance, appears to have a superior combination of properties as compared with other high strength steels. Selected comparisons have been published by the alloy producer. (Ref. 16)

1.1 Commercial Designation - AerMet 100

1.2 Alternate Designations - UNS K92580

1.3 Specifications

1.3.1 *[Table]* AMS Specifications

1.4 Composition

1.4.1 *[Table]* Chemical Composition

1.5 Heat Treatment

1.5.1 *[Table]* AMS specified heat treatment for specimens cut from bars and forgings with 100 sq. in. or less in cross-section

1.5.2 Annealing. 1225F to 1275F, 16 hours. Annealing at lower temperatures can result in retained austenite.

1.5.3. Normalize. 1650F, 1 hour, Air Cool

1.5.4 Solution treatment. 1625F, 1 hour, Air Cool or Oil Quench.

Air cooling appears to be sufficient to develop full tensile strength properties in sections up to at least 2 in. in thickness (Fig. 3.2.1.7). This air hardening is associated with a relatively low M_s temperature and a sluggish banite transformation (Fig 2.1.2.1). There appears to be essentially no difference in the tensile strength between air cooling and oil quenching over a wide range of aging temperatures (Fig. 3.2.1.4); however, the tensile yield strength of oil quenched material is lower in the aging temperature range between about 500 and 800F (which is not a normal aging range). At higher aging temperatures this difference diminishes considerably (Fig. 3.2.1.4). Water quenching is not recommended.

	Fe
3.1	Cr
11.5	Ni
13.5	Co
1.2	Mo
0.23	C

1.5.5. Refrigeration. To ensure the transformation of retained austenite, refrigeration at -100F following solution treatment is recommended.

1.5.6. Aging. This alloy possesses strong secondary hardening characteristics (e.g. Figs. 1.6.2 and 3.2.1.3) with peak tensile strength being developed by aging between 800 and 850F. At higher aging temperatures, the strength properties decrease rapidly with a corresponding increase in impact energy and fracture toughness (Figs. 3.2.3.1 and 3.2.7.2.1). Aging temperatures less than 875F are not recommended. From the limited amount of information on aging time (Fig. 3.2.1.6) it appears that aging at 900F in excess of about 6 hours can produces a loss in tensile strength properties.

1.5.7 Stress relief anneal. 800F 1 to 3 hrs, Air Cool

1.5.8 Snap temper. 400F 5 hrs (to permit straightening prior to aging)

1.6 Hardness

Annealed (Overaged) - 37 to 39 R_C (Ref.16)

1.6.1 *[Figure]* Effect of aging temperature on hardness of forging

1.6.2 *[Figure]* Effect of aging temperature on hardness of specimens cut from 10-inch-diameter bar

1.7 Forms and Conditions Available

Bars, Forgings, Plate, Strip, Wire, Castings

1.8 Melting and Casting Practice

Vacuum Induction Melt + Vacuum Arc Remelt

Preliminary development work indicates that the alloy can be vacuum cast and hot isostatically pressed (HIP) to yield mechanical properties equal to the wrought product (Table 1.8.1).

1.8.1 *[Table]* Mechanical properties of vacuum cast and HIP'ed samples

1.9 Special Considerations

1.9.1 The fracture toughness is very sensitive to the aging temperature at temperatures below about 900F and aging below 875F is not recommended (Fig. 3.2.7.2.1).

This section produced with the support of NASA-Lewis Research Center.

1.9.2. In common with other ultra high strength steels, the impact energy (Fig. 3.2.3.2) and, probably, the fracture toughness is substantially reduced at very low temperatures.

1.9.3. Inadequate cooling rates from the solution temperature can result in mixed structures containing banite which will increase the strength and reduce the fracture toughness. An indication of such an effect is shown in Fig. 3.2.7.2.3, although these data are insufficient to establish the limiting thickness for air cooling.

1.9.4 Long time elevated temperature exposure at 700F produces small increases in the ultimate tensile and yield strength (compare Figs. 3.3.1.1 and 3.3.1.2) and a substantial reduction in the Charpy V impact energy at 400F (Fig. 3.3.3.1). The fracture toughness (Table 3.2.7.2.4) is also reduced by this 700F exposure. The extent of elevated temperature exposure effects and their mechanisms are unknown at this time.

1.9.5 Decarburization will occur when air exposure exceeds 1000F (Ref. 16)

1.9.6 Water quenching should be avoided because quench cracking may occur in regions having sharp changes in crossection.

1.9.7 Retained austenite increases rapidly with increase in aging temperature above 900F (Fig. 1.9.7.1).

1.9.7.1 *[Figure]* Retained austenite as a function of aging temperature

2. Physical Properties and Environmental Effects

2.1 Thermal Properties

2.1.1 Melting Range. Heating - solidus, 2614F
liquidus, 2729F
Cooling - solidus, 2633F

2.1.2 Phase Changes. A detailed TEM analysis of the hardening phenomena in this alloy (Ref. 14) revealed the phase changes responsible for the variation in mechanical properties with heat treatment. These are briefly summarized as follows. The as-quenched and cryogenically treated alloy was completely martensitic with a mixture of lathes and plates coupled with a high dislocation density. A fine dispersion of spherical complex carbide particles was also present. The amount of retained austenite was extremely small (< 1 percent). Aging at 800F results in the formation of a relatively coarse Fe_3C Widmanstaten structure within the lathes and elongated carbides at lath and twin boundaries. This structure had a low fracture toughness (Fig. 3.2.7.2.1). With further aging at 850F these carbides were largely replaced by extremely fine needle-shaped precipitates coherent with the matrix and corresponding to the peak in secondary hardening. (The composition of the needles could not be identified.) Further aging at 900F produced coarsening of the needle-shaped precipitates, corresponding to the rapid development of overaging and high fracture toughness (Figs. 3.2.1.3 and 3.2.7.2.1). Reverted austenite formation was also present at the lath boundaries for the 900F age. Further aging (950 to 1050F) produced additional precipitate coarsening, loss of matrix precipitate coherency, and increasing amounts of reverted austenite. The precipitates contained in the structures produced by aging at 900 F and above were identified as M_2C carbides containing Cr, Mo, and Fe.

2.1.2.1 *[Figure]* Continuous cooling curves from solution treatment at 1625F

2.1.2.2 Transformation temperatures - A_{c1} = 1065F; A_{c3} = 1525F (Ref. 11)

2.1.3 Thermal Conductivity

2.1.3.1 *[Figure]* Thermal conductivity of annealed bar

2.1.4 Thermal Expansion

2.1.4.1 *[Figure]* Mean coefficient of linear thermal expansion for annealed or solution treated and aged bar

2.1.5 Specific Heat.

2.1.5.1 *[Figure]* Specific heat of rolled bar

2.1.6 Thermal Diffusivity.

2.1.6.1 *[Figure]* Thermal diffusivity of annealed bar

2.2. Other Physical Properties

2.2.1 Density. 0.285 lbs/in.^{3}

2.2.2 Electrical Properties.

2.2.3 Magnetic Properties.

2.2.3.1 *[Figure]* DC normal induction curve for heat treated alloy

2.2.4 Emittance.

2.2.5 Damping Capacity.

2.3 Chemical Environments

2.3.1 General Corrosion.

2.3.2 Stress Corrosion. (see also Figs. 3.5.3.2 to 3.5.3.6) At the time this Chapter was prepared, the only available data were the results from notch tensile specimens subjected to alternate immersion in 3.5 percent NaCl solution and the effects of stress intensity level on failure time in 3.5 percent NaCl solution using precracked, cantilever loaded beam specimens. One purpose of these tests was to establish a stress level or K level (K_{Iscc}) below which no failure would occur in the test environment. The data at hand do not establish these levels. None of the alternate immersion specimens failed (Table 2.3.2.2) and the cantilever bend specimens (Fig. 2.3.2.1) did not establish a K_{Iscc}.

However, the data may be useful for comparative purposes. Thus, AerMet 100 appears to be more resistant to stress corrosion in 3.5 percent NaCl than 300 M (Fig. 2.3.2.1).

2.3.2.1 *[Figure]* Effect of applied stress intensity factor on the failure time of AerMet 100 and 300 M forgings in 3.5 percent NaCl solution

2.3.2.2 *[Table]* Results for notch tensile specimens subjected to steady stress and alternate immersion in 3.5 percent NaCl solution

2.4 Nuclear Environments

3 Mechanical Properties

3.1 Specified Mechanical Properties

3.1.1 *[Table]* AMS minimum properties for bar and forgings aged at 900 F or 875F

3.2 Mechanical Properties at Room Temperature

3.2.1 Tensile Stress-Strain Diagrams and Tensile Properties

3.2.1.1 *[Figure]* Typical tensile stress-strain curve for longitudinal and short-transverse directions

3.2.1.2 *[Figure]* Effect of aging temperature on the tensile properties of forgings for specimens air cooled or oil quenched from the solution temperature

3.2.1.3 *[Figure]* Effect of aging temperature on transverse tensile properties of 10-inch-diameter forging

3.2.1.4 *[Figure]* Effect of aging temperature on the longitudinal tensile properties of forging for specimens air cooled or oil quenched from the solution temperature

3.2.1.5 *[Table]* Effect of aging temperature on the tensile properties and plane strain fracture toughness of specimens cut from two sizes of forgings from a single heat (No. 88287)

3.2.1.6 *[Figure]* Effect of aging time on specimens cut from forgings: one oil quenched from solution temperature, the other gas quenched (< 400F within 20 min.) in vacuum furnace (Data from two suppliers)

3.2.1.7 *[Figure]* Effect of heat-treated section size on the tensile properties of specimens cut from 10-inch-diameter die forged billet

3.2.1.8 *[Table]* Longitudinal and transverse tensile properties of specimens aged at 875F which were cut from various forgings representing seven heats

3.2.1.9 *[Table]* Longitudinal and transverse tensile properties of specimens aged at 900F which were cut from various forgings representing four heats

3.2.1.10 *[Table]* Tensile properties, plane strain fracture toughness, Charpy V energy, and hardness of specimens removed from production landing-gear piston/axle forging

3.2.2 Compression Stress-strain Diagrams and Compression Properties

3.2.2.1 *[Figure]* Typical compression stress-strain curve for longitudinal and short-transverse directions

3.2.2.2 *[Table]* Longitudinal and transverse compression yield strengths of specimens aged at 875F which were cut from various size forgings representing seven heats

3.2.2.3 *[Table]* Longitudinal and transverse compression yield strengths of specimens aged at 900F which were cut from various size forgings representing four heats.

3.2.3 Impact. (see also Table 3.2.1.10)

3.2.3.1 *[Figure]* Effect of aging temperature on Charpy V impact energy of forging for specimens air cooled or oil quenched from the solution temperature

3.2.3.2 *[Figure]* Effect of aging temperature on Charpy V energy of specimens air cooled or oil quenched from the solution temperature

3.2.4 Bending.

3.2.5 Torsion and Shear.

3.2.5.1 *[Table]* Longitudinal and transverse shear strength of specimens aged at 875F which were cut from various size forgings representing seven heats

3.2.5.2 *[Table]* Longitudinal and transverse shear strength of specimens aged at 900F which were cut from various size forgings representing four heats

3.2.6 Bearing.

3.2.6.1 *[Table]* Longitudinal bearing yield and ultimate strengths of specimens aged at 875F which were cut from various size forgings representing seven heats

3.2.6.2 *[Table]* Longitudinal bearing yield and ultimate strengths of specimens aged at 900F which were cut from various size forgings representing four heats

3.2.7 Stress Concentration.

3.2.7.1 Notch Properties

3.2.7.2 Fracture Toughness (see also Tables 3.1.1, 3.2.1.5, and 3.2.1.10 and Section 1.9)

3.2.7.2.1 *[Figure]* Effect of aging temperature on plane strain fracture toughness of forging for specimens air cooled or oil quenched from the solution temperature

3.2.7.2.2 *[Table]* Plane strain fracture toughness of specimens aged at 875F which were cut from various forgings representing seven heats

3.2.7.2.3 *[Figure]* Effect of heat treated section thickness on plane strain fracture toughness of specimens cut from a 10-in.-diameter forged billet

3.2.7.2.4 *[Table]* Effect of 700F, 3000-hour air exposure on the plane strain fracture toughness of specimens cut from forging

3.2.8 Combined Loading

3.3 Mechanical Properties at Various Temperatures

3.3.1. Tension Stress-strain Diagrams and Tensile Properties

3.3.1.1 *[Figure]* Effect of elevated test temperature on tensile properties of a forging aged at 900F

3.3.1.2 *[Figure]* Effect of test temperature on tensile properties following 700F, 3000-hour air exposure for a forging aged at 900F

3.3.2 Compression Stress-strain Diagrams and Compression Properties

3.3.3 Impact.

3.3.3.1 *[Figure]* Effect of test temperature on Charpy V impact energy for specimens cut from forging with and without a prior 700F, 3000-hour air exposure

3.3.3.2 *[Figure]* Effect of cryogenic and elevated temperature on the Charpy V impact energy of specimens from a 10-in.-diameter round forging and aged at several temperatures

3.3.3.3 *[Figure]* Cooling curves for tensile and Charpy V specimens cooled in vermiculite following solution treating to simulate the cooling rate of 1-in.-thick CT K_{Ic} specimens cooled in still air

3.3.4 Bending.

3.3.5 Torsion and Shear.

3.3.6 Bearing.

3.3.7 Stress Concentration.

3.3.7 Notch Properties.

3.3.7.1 Fracture Toughness.

3.3.8 Combined Loading.

3.4 Creep and Creep Rupture Properties

3.5 Fatigue Properties

3.5.1 Conventional High-Cycle Fatigue. The database for high cycle fatigue is small. The majority of the data relates to operational stress spectrum tests obtained for design of a landing gear/axle forging (Ref. 13). These tests involved different frequencies, many surface conditions, different R ratios and several stress concentration factors. By appropriate selection and combination of these data, it was possible to develop fatigue curves over a range of cycles from 10^3 to somewhat beyond 10^6. The results of this analysis are shown in Figs. 3.5.1.1 to 3.5.1.4 which illustrate the following:

(1) There is a negligible effect of frequency between 10 and 20 Hz. The data for 5 Hz are confined to relatively low cyclic lives but do not exhibit a frequency effect within this range .

(2) Grinding after heat treatment appears to result in somewhat higher fatigue lives than heat treating following grinding.

(3) Machining (125 rms surface finish) before heat treatment appears to yield essentially the same fatigue lives as grinding (63 rms surface finish) before heat treatment.

(4) Large improvements in fatigue lives are produced by shot peening when applied to ground or machined surfaces and these improvements are retained when chrome plating followed by grinding is applied to the shot peened surface.

(5) Consistent with an expected trend, fatigue lives at R= - 0.33 appear to be somewhat longer than at R = -1.

Recognizing that the database is small, an attempt was made to estimate the maximum stresses for 10^6 cycles. The results are shown in Table 3.5.1.5. It was not possible to incorporate the data shown in Fig. 3.5.1.6 in these estimates because attempts to discover the details of the test conditions were not successful.

3.5.1.1 *[Figure]* Axial load fatigue data at R = - 1 for smooth specimens cut from a forging and tested with various surface conditions at different frequencies

3.5.1.2 *[Figure]* Axial load fatigue data at R = - 1 and K_t = 3 for specimens cut from a forging and tested with various surface conditions at different frequencies

3.5.1.3 *[Figure]* Axial load fatigue data at R = - 0.33 for smooth specimens cut from a forging and tested with various surface conditions at different frequencies

3.5.1.4 *[Figure]* Axial load fatigue data at R = - 0.33 and K_t = 3 for specimens cut from a forging and tested with various surface conditions and at different frequencies

3.5.1.5 *[Table]* Estimates of the fatigue strength at 10^6 cycles for axial loading of specimens from a landing-gear piston/axle forging

3.5.1.6 *[Figure]* Fatigue data for forgings tested at R = 0 using smooth and notched specimens of unspecified geometry

3.5.1.7 *[Figure]* Torsional fatigue strength at 400F of AerMet 100 and 250 Grade Maraging steel.

3.5.2 Low Cycle Fatigue.

3.5.2.1 *[Figure]* Low cycle fatigue data for crack initiation and failure for specimens cut from a forging.

3.5.3 Fatigue Crack Propagation. As expected, the fatigue crack growth rates are relatively insensitive to the R ratio in the sector where there is a nearly linear relation between log da/dN and log ΔK. In this region, negligible influence of the 3.5 percent NaCl environment is observed. In the region of very low growth rates, K_{th} increases with the R ratio for both the neutral environment and for the 3.5 percent NaCl solution. It is interesting to note that the K_{th} values are higher for the more corrosive NaCl environment. This effect was attributed to corrosion- controlled crack closure (Ref. 7).

3.5.3.1 *[Figure]* Fatigue crack propagation rates in air at several R values for a landing-gear piston/axle forging

3.5.3.2 *[Figure]* Fatigue crack growth rates at R = 0.1 in 3.5 percent NaCl and in dry nitrogen for a forged slab

3.5.3.3 *[Figure]* Fatigue crack growth rates at R = 0.1 for AerMet 100 in dry nitrogen and 300 M in air

3.5.3.4 *[Figure]* Fatigue crack growth rates at R = 0.1 for AerMet 100 and 300 M in 3.5 percent NaCl

3.5.3.5 *[Figure]* Fatigue crack growth rates at R = 0.5 in 3.5 percent NaCl and in dry nitrogen for a forged slab

3.5.3.6 *[Figure]* Fatigue crack growth rates at R = 0.8 in 3.5 percent NaCl and in dry nitrogen for a forged slab

3.6 Elastic Properties

3.6.1 Poisson's Ratio.

3.6.2 Modulus of Elasticity.

3.6.2.1 *[Table]* Tension and compression moduli of elasticity determined for specimens aged at 875F which were cut from various size forgings representing seven heats

3.6.3 Modulus of Rigidity.

3.6.4 Tangent Modulus.

3.6.5 Secant Modulus.

4 Fabrication

4.1 Forming

4.1.1 Forging. Preliminary breakdown - 2150F max.
Finish - 1800F to below 1650F (Ref. 16)

4.2 Machining and Grinding

Normally, machining should be done in the annealed condition which provides a hardness of 37 to 39 R_C. At lower hardnesses, machining is more difficult due to the production of long string-like chips which clog the cutting tools (Ref. 16). In comparative machining tests using various processes, it was reported that AerMet 100 was more difficult to machine at hardnesses of R_C 40 and R_C 53 than was 300 M at the same hardness levels (Ref. 13).

4.3 Joining

4.3.1 Welding. The preliminary results of welding studies that are in progress (August 1995) indicate that the alloy can be welded by the electron beam, cold-wire-feed plasma arc, and GTA processes. Relatively low heat input, multiple pass welds produce the best results. Tensile and impact data are available for GTA welds in plate (Table 4.3.1.1). Of the various pre- and post-heat treatments studied, Condition A (welding annealed material followed by normalizing and reannealing prior to solution treating and aging) produced tensile properties exceeding the minimums specified in AMS 6532 (Table 3.1.1). The remaining conditions did not produce welds meeting the AMS minimum property requirements. The weld impact energies differed little for the various conditions and, in all cases, were well below the values reported for parent material (See Fig. 3.2.3.2) in laboratory tests, but, for Conditon A were close to those reported for specimens removed from production forged parts (see Tale 3.2.1.10). It should be noted that relatively low impact values may not reflect correspondingly low plane strain fracture toughness. For example, Table 3.2.1.10 shows a mean K_{Ic} value of 107.2 ksi$\sqrt{in}$. with a mean impact value of 29.7 ft-lbs.

4.3.1.1 *[Table]* Preliminary results (duplicate tests) for tensile properties and Charpy V impact energies for GTA welds in plate

4.4 Surface Treating

The alloy can be nitrided.

Table 1.3.1 AMS Specifications (Refs. 3, 15)

Alloy	AerMet 100
Form	Bars and Forgings
Specifications	Coverage
AMS 6478	Vacuum Melted, Annealed Heat Treatable to 290 ksi (1999 Mpa) Tensile Strength
AMS 6532	Vacuum Melted, Annealed

Table 1.4.1 Chemical composition (Refs. 3, 15)

Alloy	AerMet 100	
Source	AMS 6478 and 6532	
Composition	Percent	
Element	Minimum	Maximum
C	0.21	0.25
Mn		0.10
Si		0.10
P		0.008
S		0.005
P + S		0.010
Cr	2.9	3.3
Ni	11.0	12.0
Co	13.0	14.0
Mo	1.10	1.30
Ti		0.015
Al		0.015
O_2		20 ppm
N_2		15 ppm

Table 1.5.1 AMS specified heat treatment for specimens cut from bars and forgings with 100 sq. in. or less in cross-section.

Alloy	AerMet 100			
Source	AMS 6532 (Ref. 15)		AMS 6478 (Ref. 3)	
Solution Treat	1600F to 1650F, 60 to 75 minutes			
Quench				
t =< 1.25 in.	Air Cool (AC)			
t > 1.25 in.	Oil Quench (OQ)			
Refrigerate	-85 to -115F, 55 to 65 minutes, Air Warm			
Age	890 to 910F, 5 to 8 hrs, AC		865 to 885F, 5 to 8 hrs, AC	
Form	Bars	Forgings	Bars	Forgings
Anneal	1115 to 1250F, 8 hrs min, AC	1225 to 1275F, 8 hrs min, Fan Cool	1225 to 1275F, 16 hrs min, AC	1225 to 1275F, 8 hrs min, Fan Cool
Normalize	-	1225 to 1275F, 55 to 75 minutes, AC	-	1225 to 1275F, 55 to 75 minutes, AC

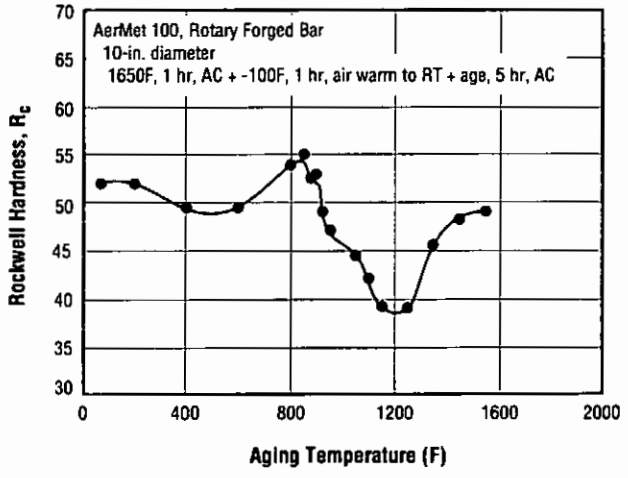

Figure 1.6.1 Effect of aging temperature on hardness of forging (Ref. 5)

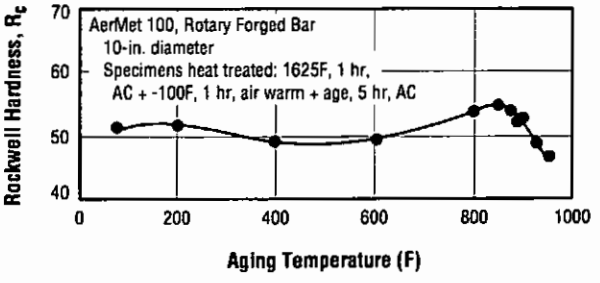

Fig. 1.6.2 Effect of aging temperature on hardness of specimens cut from 10-inch-diameter bar (Ref. 5)

Table 1.8.1 Mechanical properties of vacuum cast and HIP'ed samples (Ref. 18)

Alloy	AerMet 100	
Form	Castings	
HIP Cycle in Argon	1550F, 1 hr., heat to 2250F, 6.5 hr. at 30 ksi pressure, FC	
Heat Treatment	1250F, 16 hr., Cool 600F per hr. to RT + 1650F, 1 hr., AC + -100F, 1 hr., Air Warm to RT + 900F, 5 hr., AC	
Sample	1	2
F_{tu} (ksi)	277	292
F_{ty} (ksi)	242	249
Elongation, E (percent)	12.4	13
Reduction in Area, RA (percent)	57	58
Fracture Toughness, K_{Ic} (ksi $\sqrt{in.}$)	113	118
Charpy V Impact Energy (ft-lb)	26	25

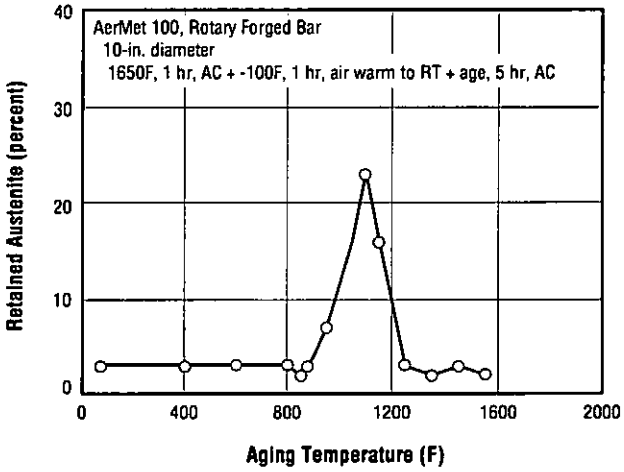

Figure 1.9.7.1 Retained austenite as function of aging temperature (Ref. 5)

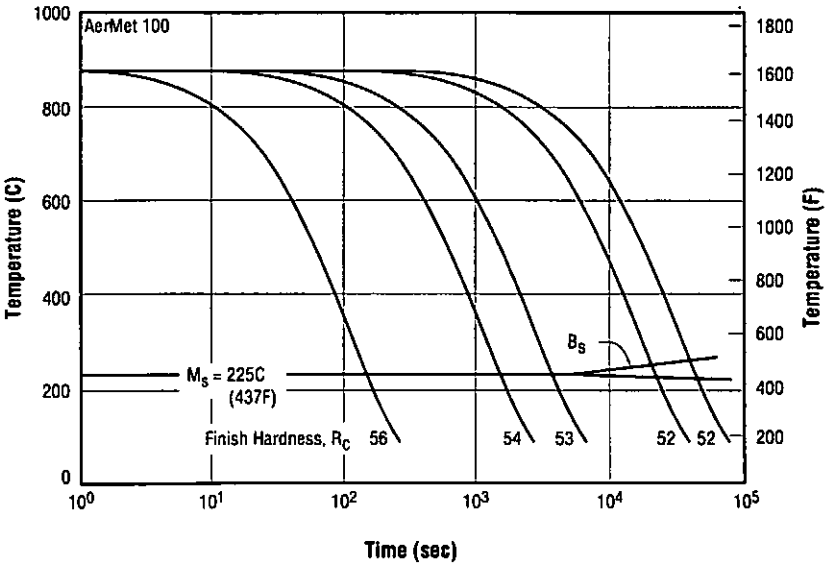

Fig. 2.1.2.1 Continuous cooling curves from solution treatment at 1625F [M_s - Martensite start (1 percent transformation); B_s - Banite start] (Ref. 2)

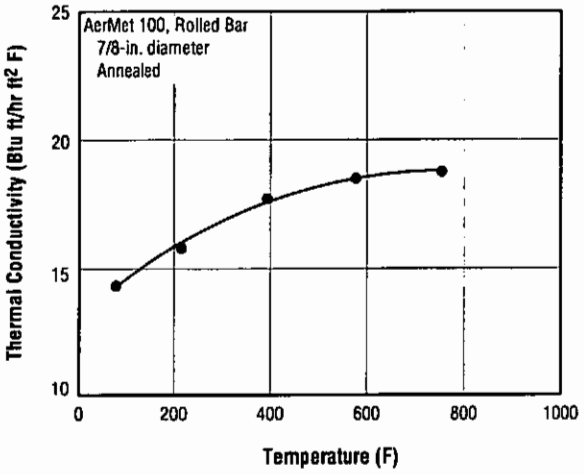

Figure 2.1.3.1 Thermal conductivity of annealed bar (Ref. 10)

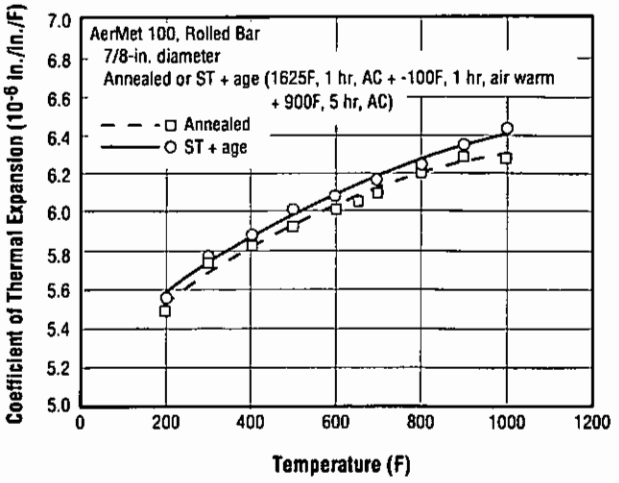

Fig. 2.1.4.1 Mean coefficient of linear thermal expansion for annealed or solution treated and aged bar (Ref. 11)

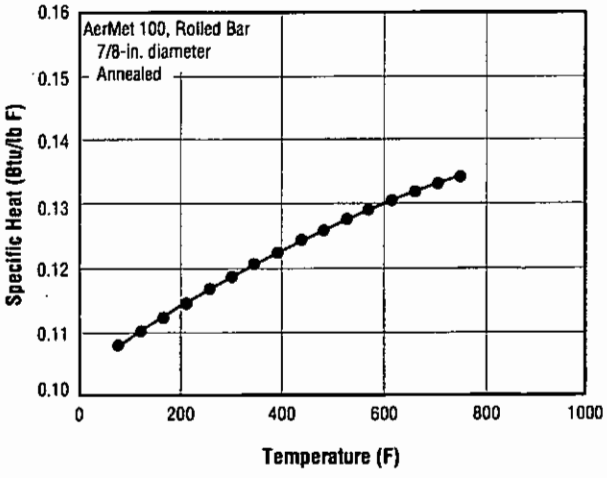

Fig. 2.1.5.1 Specific heat of rolled bar (Ref. 10)

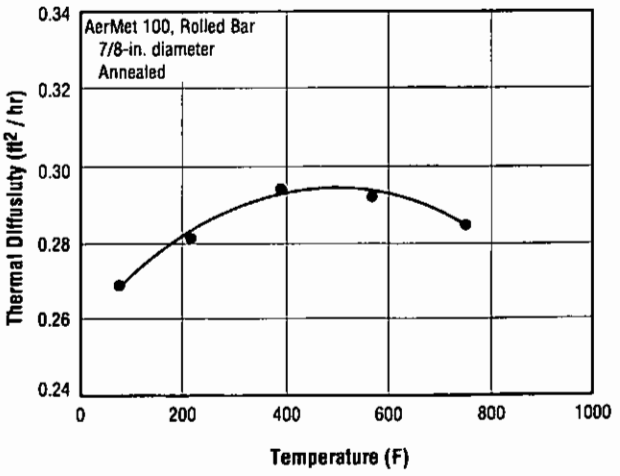

Fig. 2.1.6.1 Thermal diffusivity of annealed bar (Ref. 10)

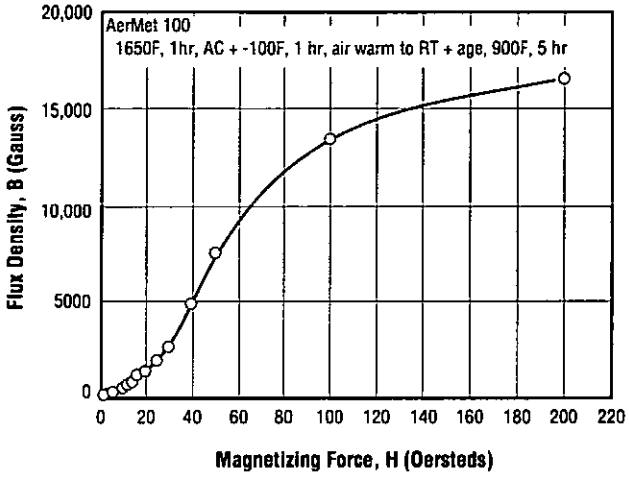

Fig. 2.2.3.1 DC normal induction curve for heat treated alloy (Ref. 2)

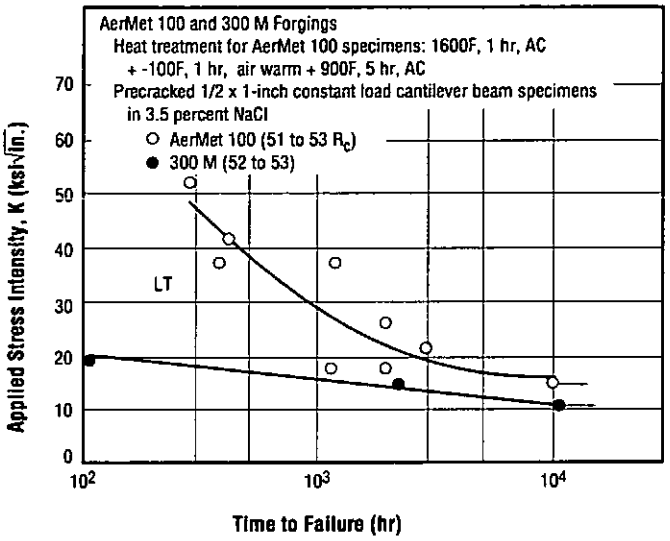

Figure 2.3.2.1 Effect of applied stress intensity factor on the failure time of AerMet 100 and 300 M forgings in 3.5 percent NaCl solution (Ref. 4)

Table 2.3.2.2 Results for notch tensile specimens subjected to steady stress and alternate immersion in 3.5 percent NaCl solution (Ref. 13)

Alloy	AerMet 100		
Form	5 to 6-in.-dia. Landing-Gear Piston/Axle Forging		
Specimen Condition	1625F, 1 hr., OQ + -100F, 1 hr., Air Warm + 900F, 4 hr.		
Environment	Alternate Immersion in 3.5 percent NaCl		
K_t	1	2	3
Stress Range (ksi)	220	240	
Exposure Time (hr)	90		
Failures	None		

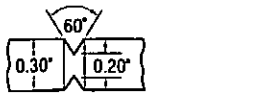

Notch radius = 0.031 in. for K_t = 2
= 0.01 in. for K_t = 3

Table 3.1.1 AMS minimum properties for bars and forgings aged at 900F or 875F (Refs. 3, 15)

Alloy	AerMet 100			
Form	Bars and Forgings			
Size[a]	≤ 100 sq in. cross-sectional area			
Source	AMS 6532		AMS 6478	
Condition[b]	ST + 900F Age		ST + 875F Age	
Direction[c]	L	T	L	T
F_{tu}, min (ksi)	280		290	
F_{ty}, min (ksi)	235	233	245	
Elongation, e, min (percent)	10	8	10	8
Reduction in Area, RA, min (percent)	55	45	50	35
Hardness, min (R_C)	53			
Fracture Toughness[d], K_{Ic} (ksi$\sqrt{in.}$) LS or LR Orientations	100		80	

[a] Properties of products > 100 sq in. cross-sectional area to be agreed upon by purchaser and vendor.

[b] For heat treatment details, see Table 1.5.1.

[c] If transverse tensile properties are measured, longitudinal properties are not required.

[d] For products < 3 in., fracture toughness measurement method and minimum values are to be agreed upon by the purchaser and the vendor.

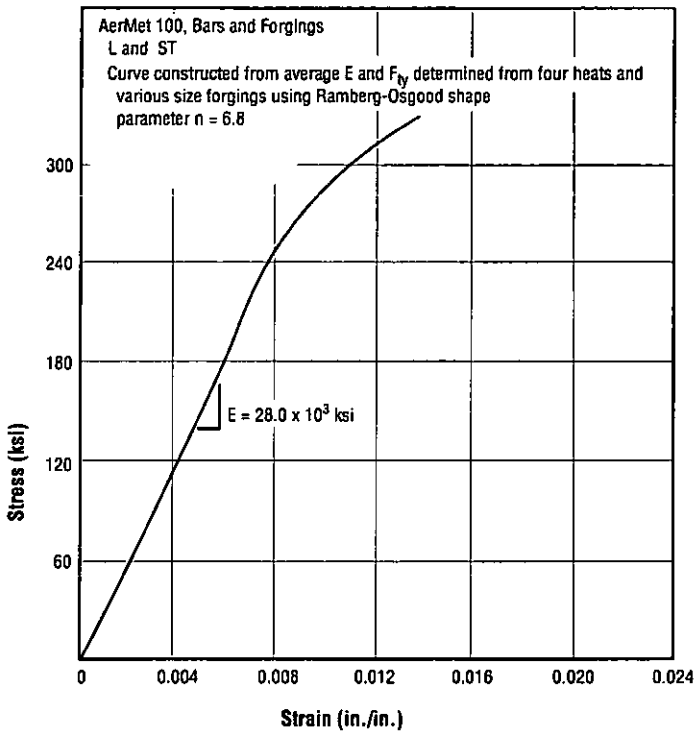

Figure 3.2.1.1 Typical tensile stress-strain curve for longitudinal and short-transverse directions (Refs. 1, 4)

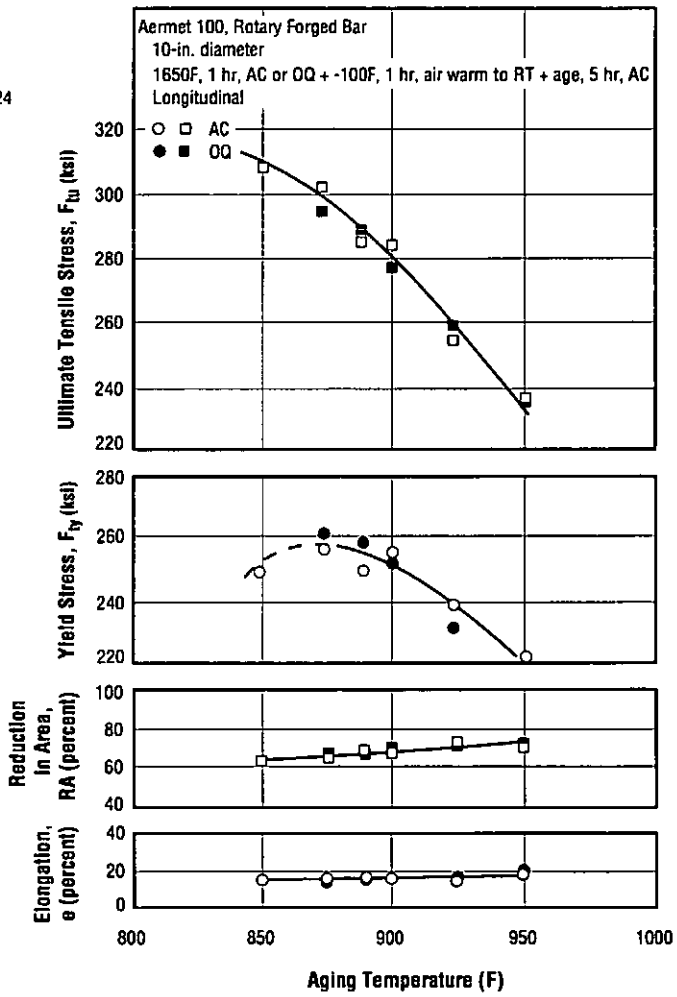

Figure 3.2.1.2 Effect of aging temperature on the tensile properties of forgings for specimens air cooled or oil quenched from the solution temperature (Ref. 5)

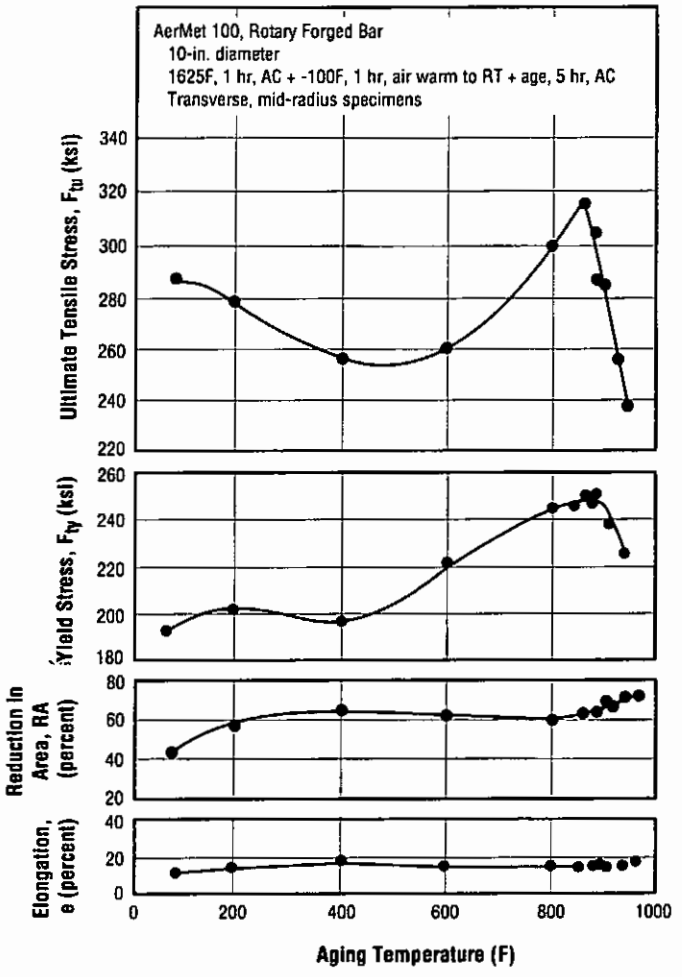

Figure 3.2.1.3 Effect of aging temperature on transverse tensile properties of 10-inch diameter forging (Ref. 8)

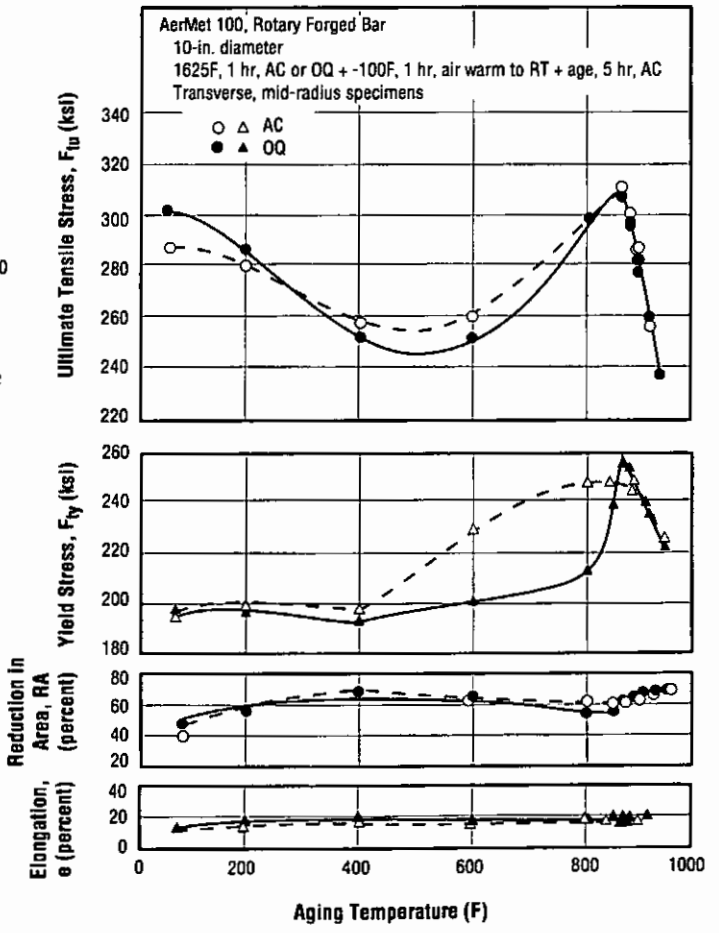

Figure 3.2.1.4 Effect of aging temperature on the longitudinal tensile properties of forging for specimens air cooled or oil quenched from the solution temperature (Ref. 5)

Table 3.2.1.5 Effect of aging temperature on the tensile properties and plane strain fracture toughness of specimens cut from two sizes of forgings from a single heat (No. 88287) (Refs. 2, 6)

Alloy	AerMet 100			
Form	Forgings			
Source	Ref. 2		Ref. 6	
Condition	1625F, 1 hr., OQ + -100F, 1 hr., + Age, 5 hr.			
5 hr. Aging Temperature (F)[c]	875		900	
Size	5 x 8 in.		16-in DOC[a]	
Direction[b]	L	T	L	T
F_{tu}, min (ksi)[c]	302	301	287	289
F_{ty}, min (ksi)	259	258	249	252
Elongation, e (percent)	15	13	16.6	16
Reduction in Area, RA (percent)	66	58	68	59
Fracture Toughness[d], K_{Ic} (ksi$\sqrt{in.}$)	90	78	113	115

[a] Double octagon (16-sided) press forging.

[b] L - Loading axis parallel to grain flow; T - Loading axis normal to grain flow.

[c] Average of duplicate tensile results for the 5 x 8-in. forging; Average of 10 tensile results for the 16-in. DOC.

[d] Average of triplicate toughness results for the 5 x 8-in. forging; Average of five toughness results for the 16-in. DOC.

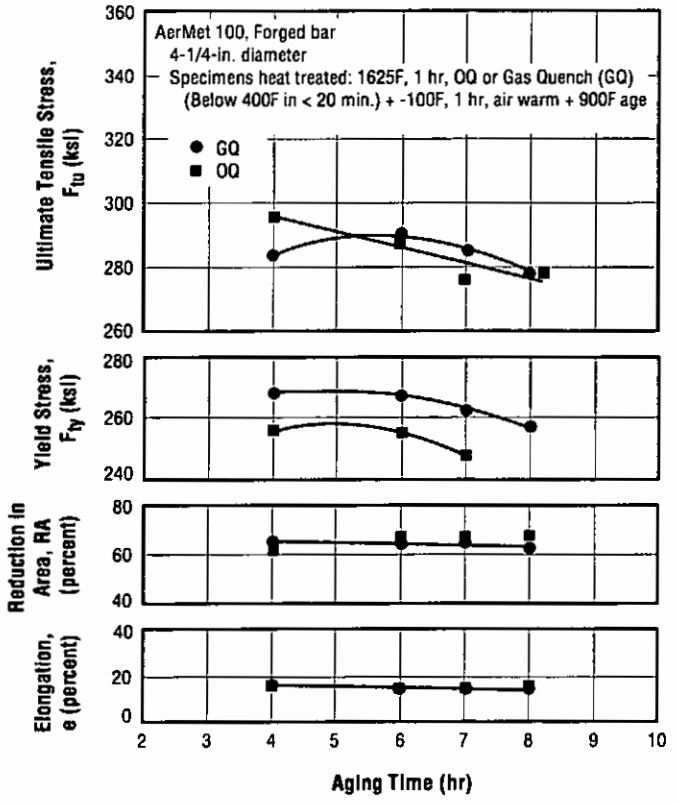

Figure 3.2.1.6 Effect of aging time on specimens cut from forging: one oil quenched from solution temperature, the other gas quenched (< 400F within 20 min.) in vacuum furnace (Data from two suppliers) (Ref. 13)

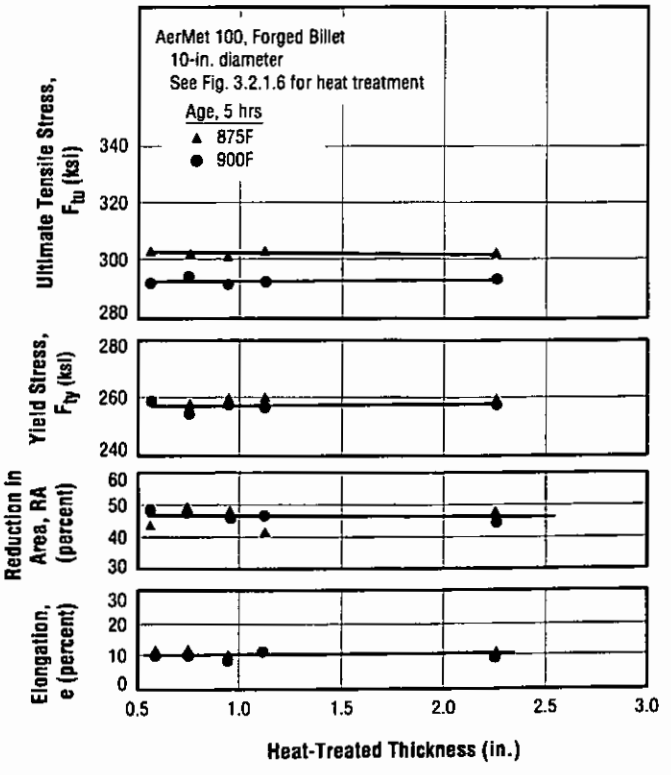

Fig. 3.2.1.7 Effect of heat-treated section size on the tensile properties of specimens cut from 10-inch-diameter die forged billet (Ref. 13)

Table 3.2.1.8 Longitudinal and transverse tensile properties of specimens aged at 875F which were cut from various forgings representing seven heats (Ref. 2)

Alloy	AerMet 100			
Form	Forgings			
Sizes (in.)	Rounds (3, 3.5, 4.25, 5, 6, and 8) Round-cornered square (5 and 7.25) Rectangle (5 x 8)			
Condition	1600 to 1650 in salt, 60 to 75 min, AC + -85 to -115F, 55 to 65 min, Air Warm + 865 to 885F, 5 hr,			
Sampling	D/4 or t/4 locations; 2 specimens from each forging			
	Longitudinal[a]			
	F_{ty} (ksi)	F_{tu} (ksi)	Elongation, e (percent)	Reduction in Area, RA (percent)
Low	251	296	13	58
High	265	307	16	66
Mean	258	302	14.2	64
Standard Deviation	3.9	2.4	0.8	2.3
	Transverse[a, b]			
Low	250	298	10	42
High	268	307	13	61
Mean	259	302	12	50
Standard Deviation	4.7	2.3	1.0	4.9

[a] Results shown for 20 specimens.

[b] For all sizes, loading axis was normal to grain flow.

Table 3.2.1.9 Longitudinal and transverse tensile properties of specimens aged at 900F which were cut from various forgings representing four heats (Ref. 4)

Alloy	AerMet 100			
Form	Forgings			
Sizes (in.)	Rounds (3, 4-5/8, 5, 6, 6-1/2, 8-1/2, and 10) Rectangle (7-1/4 x 7-1/4 and 5 x 8)			
Condition	1600 to 1650 in salt, 60 to 75 min, AC + -85 to -115F, 55 to 65 min, Air Warm + 890 to 910F, 5 to 8 hr, AC			
Sampling	D/4 or t/4 locations; 2 specimens from each forging			
	Longitudinal[a]			
	F_{ty} (ksi)	F_{tu} (ksi)	Elongation, e (percent)	Reduction in Area, RA (percent)
Low	235	280	14	58
High	266	293	18	71
Mean	247	287	16.1	67.3
Standard Deviation	5.9	3.5	0.7	3.3
	Transverse[a, b]			
Low	239	283	11.3	42.1
High	261	293	19.9	58.7
Mean	246	288	14.3	56.6
Standard Deviation	4.8	3.4	1.7	6.0

[a] Results shown for 20 specimens.

[b] For all sizes, loading axis was normal to grain flow.

Table 3.2.1.10 Tensile properties, plane strain fracture toughness, Charpy V energy, and hardness of specimens removed from production landing-gear piston/axle forging (Ref. 13)

Alloy	AerMet 100						
Form	5- to 6-in.-dia. landing-gear piston/axle forging						
Condition	Normalize 1650F + 1250F Overage						
Specimens	1625F, 1 hr., OQ + -100F, 1 hr., air warm + 900F, 5-1/2 hr., AC						
Direction	Transverse				L - R		
	F_{tu} (ksi)	F_{ty} (ksi)	Elongation, e (percent)	Reduction in Area, RA (percent)	K_{Ic} (ksi$\sqrt{in.}$)	Charpy V Energy (ft-lb)	Hardness, R_c
Mean	287.7	263.0	17.4	59.9	107.2	29.7	52.3
Standard Deviation	2.89	4.54	1.67	7.8	4.35	3.83	.516
Number of Tests	8				4	6	

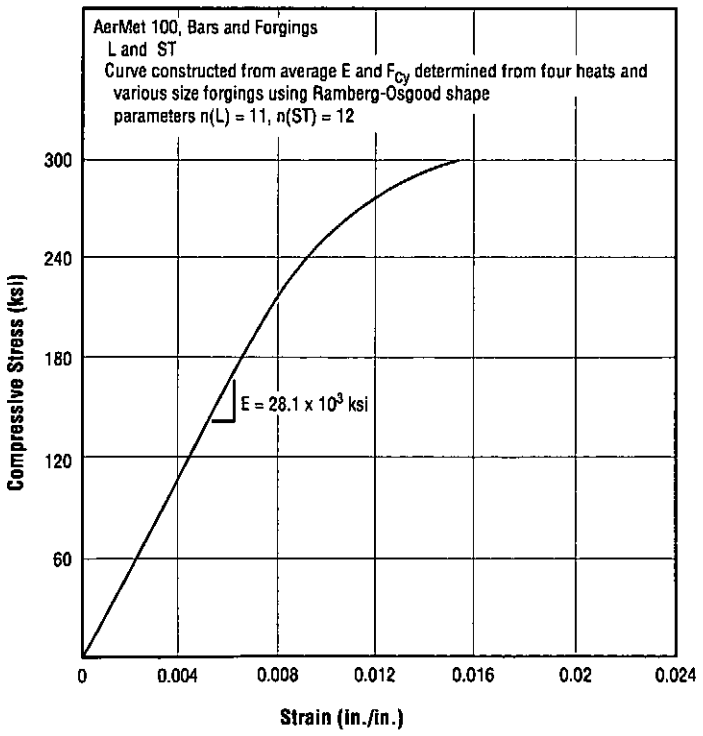

Figure 3.2.2.1 Typical compression stress-strain curve for longitudinal and short-tranverse directions (Refs. 1, 4)

Table 3.2.2.2 Longitudinal and transverse compression yield strengths of specimens aged at 875F which were cut from various size forgiings representing seven heats (Ref. 2)

Alloy	AerMet 100	
Form	Forgings	
Condition	See Table 3.2.1.8	
Sizes		
Sampling		
Direction	Longitudinal	Transverse[a]
	F_{cy} (ksi)	
No. Specimens	20	19
Low	291	291
High	301	303
Mean	297	296
Standard Deviation	3.0	3.7

[a] For all sizes, loading axis normal to grain flow.

Table 3.2.2.3 Longitudinal and transverse compression yield strengths of specimens aged at 900F which were cut from various size forgings representing four heats (Ref. 4)

Alloy	AerMet 100	
Form	Forgings	
Condition	See Table 3.2.1.9	
Sizes (in.)		
Direction	Longitudinal	Transverse[a]
	F_{cy} (ksi)	
Low	267	274
High	283	283
Mean	279	279
Standard Deviation	3.3	2.5

[a] Specimen load axis normal to grain flow.

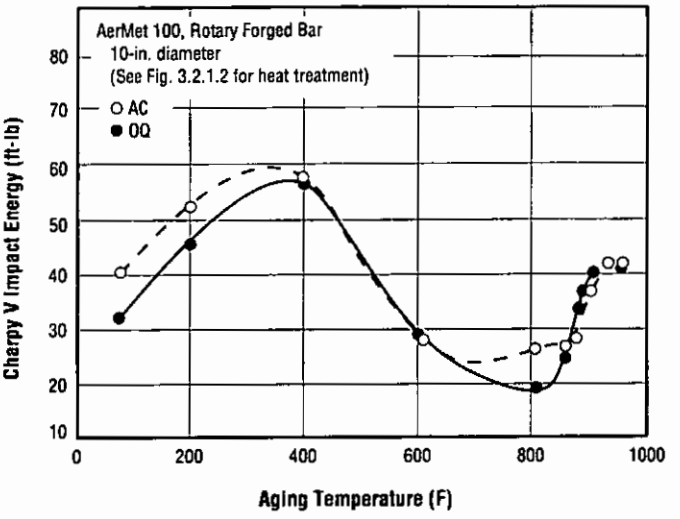

Fig. 3.2.3.1 Effect of aging temperature on the Charpy V impact energy of forging for specimens air cooled or oil quenched from the solution temperature (Ref. 5)

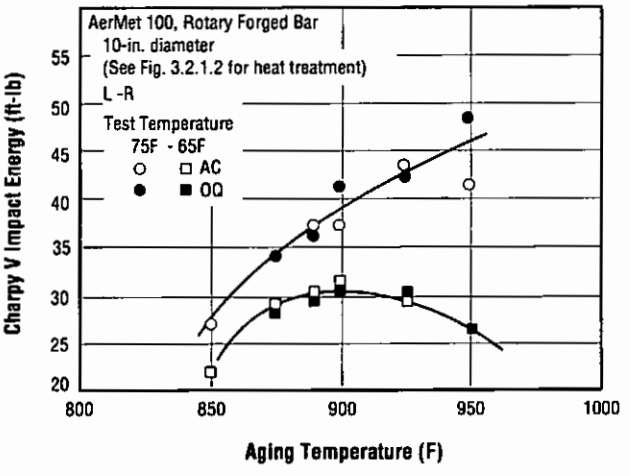

Fig. 3.2.3.2 Effect of aging temperature on Charpy V energy of specimens air cooled or oil quenched from the solution temperature (Ref. 5)

Table 3.2.5.1 Longitudinal and transverse shear strength of specimens aged at 875F which were cut from various size forgings representing seven heats (Ref. 2)

Alloy	AerMet 100	
Form	Forgings	
Condition	See Table 3.2.1.8	
Sampling		
Direction	Longitudinal	Transverse[a]
	F_{su} (ksi)	
Number of Specimens	20	
Low	189	189
High	198	210
Mean	195	198
Standard Deviation	2.3	6.0

[a] Loading axis normal to grain flow.

Table 3.2.5.2 Longitudinal and transverse shear strength of specimens aged at 900F which were cut from various size forgings representing four heats (Ref. 4)

Alloy	AerMet 100	
Form	Forgings	
Condition	See Table 3.2.1.9	
Sizes		
Sampling		
Direction	Longitudinal	Transverse[b]
Number of Specimens[a]	15	14
	F_{su} (ksi)	
Low	174	175
High	184	184
Mean	179	179
Standard Deviation	2.6	3.2

[a] Data for bent specimens excluded.

[b] Load axis normal to grain flow.

Table 3.2.6.2 Longitudinal bearing yield and ultimate strengths for specimens aged at 900F which were cut from various size forgings representing four heats (Ref. 4)

Alloy	AerMet 100			
Form	Forgings			
Condition	See Table 3.2.1.9			
Sizes				
Sampling				
Direction	Longitudinal[a]			
	F_{bry} (ksi)		F_{bru} (ksi)	
	e/D=1.5	e/D=2.0	e/D=1.5	e/D=2.0
Low	375	388	449	506
High	398	474	422	600
Mean	385	439	467	585
Standard Deviation	7.0	17.3	10.9	21.1

[a] Results shown for 20 specimens for each property.

Table 3.2.6.1 Longitudinal bearing yield and ultimate strengths of specimens aged at 875F which were cut from various size forgings representing seven heats (Ref. 2)

Alloy	AerMet 100			
Form	Forgings			
Condition	See Table 3.2.1.8			
Sizes				
Sampling				
Direction	Longitudinal[a]			
	F_{bry} (ksi)		F_{bru} (ksi)	
	e/D=1.5	e/D=2.0	e/D=1.5	e/D=2.0
Low	394	449	451	575
High	414	498	457	633
Mean	403	473	473	614
Standard Deviation	5.9	15.5	10.6	18.5

[a] Results shown for 20 specimens for each property.

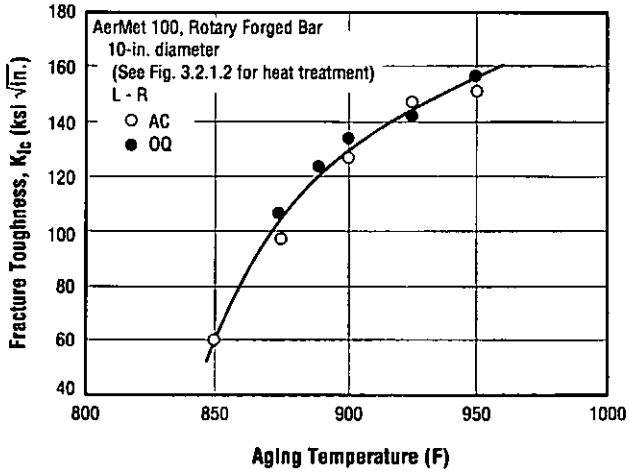

Figure 3.2.7.2.1 Effect of aging temperature on plane strain fracture toughness of forging for specimens air cooled or oil quenched from the solution temperature (Ref. 5)

Table 3.2.7.2.2 Plane strain fracture toughness of specimens aged at 875F which were cut from various forgings representing seven heats (Ref. 2)

Alloy	AerMet 100	
Form	Forgings	
Condition	See Table 3.2.1.8	
Sizes	As inTable 3.2.1.8	As in Table 3.2.1.8, except 3- and 3.5-in. rounds were not tested
Sampling	As in Table 3.2.1.8	
Number of Specimens	30	29
Crack Orientation[a]	LR or LT	CR or ST
	Fracture Toughness[b], K_{Ic} (ksi $\sqrt{in.}$)	
Low	90	73
High	110	101
Mean	99	88
Standard Deviation	6.5	8.6

[a] LR or CR applies to rounds; LT or ST applies to square or rectangular cross sections.

[b] ASTM E 399 1-inch-thick CT specimens.

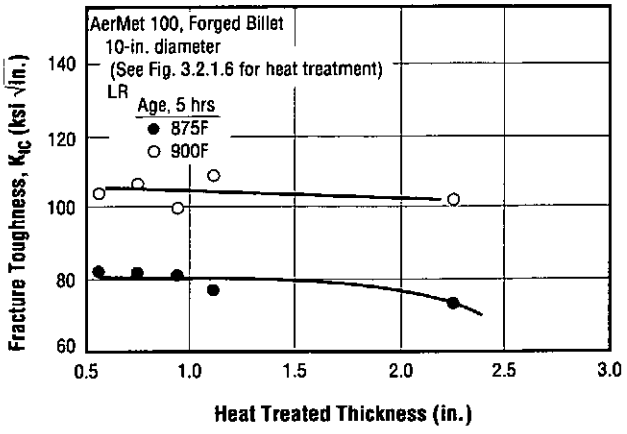

Fig. 3.2.7.2.3 Effect of heat treated section thickness on plane strain fracture toughness of specimens cut from 10-inch-diameter forged billet (Ref. 13)

Table 3.2.7.2.4 Effect of 700F, 3000-hr. air exposure on the plane strain fracture toughness of specimens cut from forging (Ref. 2)

Alloy	AerMet 100	
Form	6-in.-diameter Forging[a]	
Condition	Specimens: 1625F, 1 hr., VC[b] + -100F, 1 hr., air warm + 900F, 5 hr.	
Exposure	None	700F, 3,000 hr.
Fracture Toughness[b], K_{Ic} (ksi $\sqrt{in.}$)	97.1	83
	99.0	86.4
	100.5	

[a] Specimens cut from mid-radius.

[b] VC - Vermiculite Cooling to simulate the cooling rate of 1-in.-thick CT K_{Ic} specimens cooled in still air. See Figure 3.3.3.3.

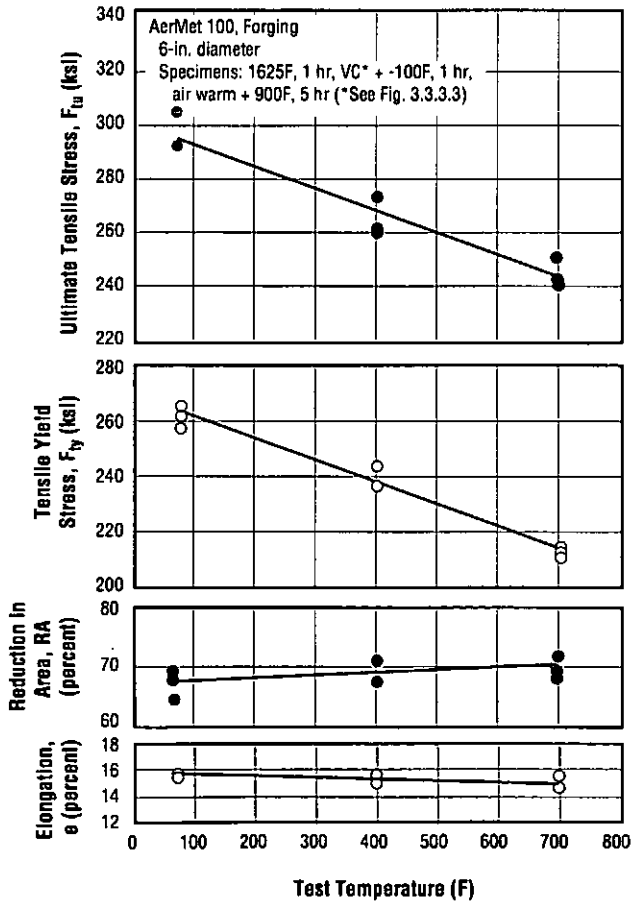

Fig. 3.3.1.1. Effect of elevated test temperature on tensile properties of a forging aged at 900F (Ref. 2)

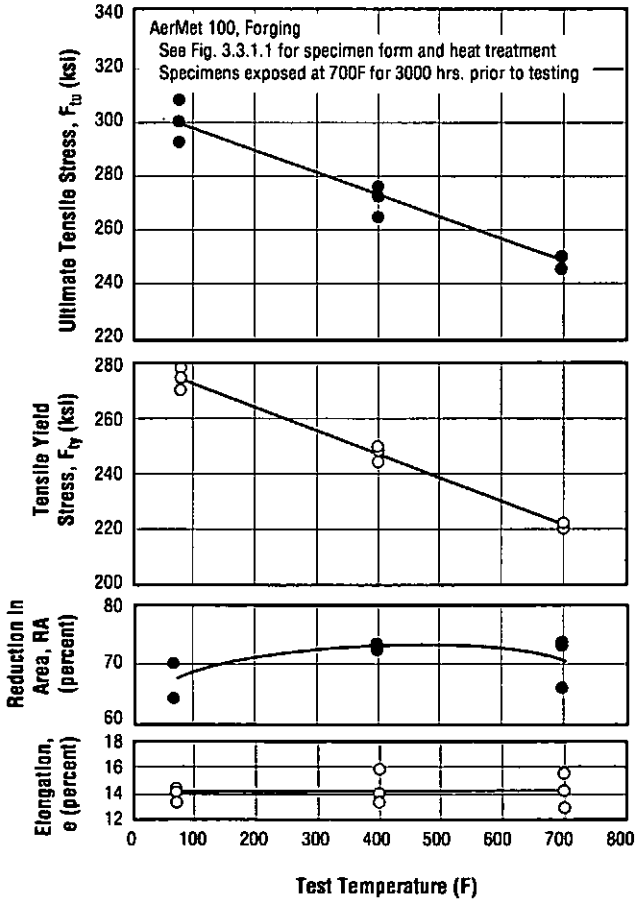

Fig. 3.3.1.2. Effect of test temperature on tensile properties following 700F, 3000 hr. air exposure for a forging aged at 900F (Ref. 2)

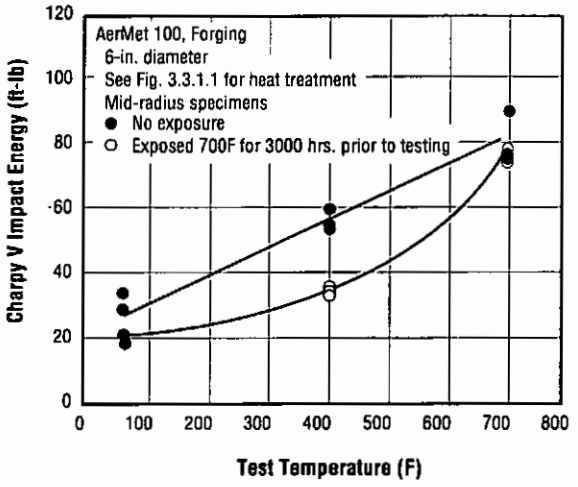

Fig. 3.3.3.1 Effect of test temperature on Charpy V impact energy for specimens cut from forging with and without a prior 700F, 3000 hr. air exposure (Ref. 2)

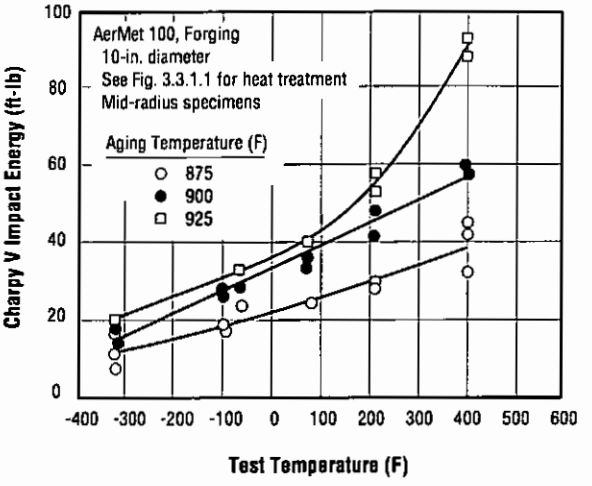

Fig. 3.3.3.2 Effect of cryogenic and elevated test temperature on the Charpy V impact energy of specimens cut from a 10-in.-diameter round forging and aged at several temperatures (Fig. 2)

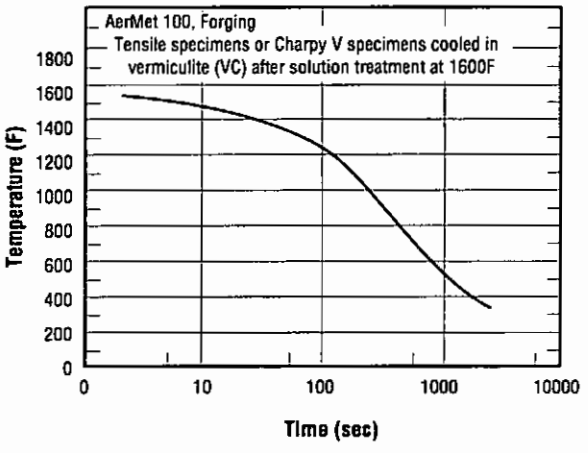

Fig. 3.3.3.3 Cooling curve for tensile and Charpy V specimens cooled in vermiculite following solution treatment to simulate the cooling rate of 1-in.-thick CT K_{Ic} specimens cooled in still air (Ref. 8)

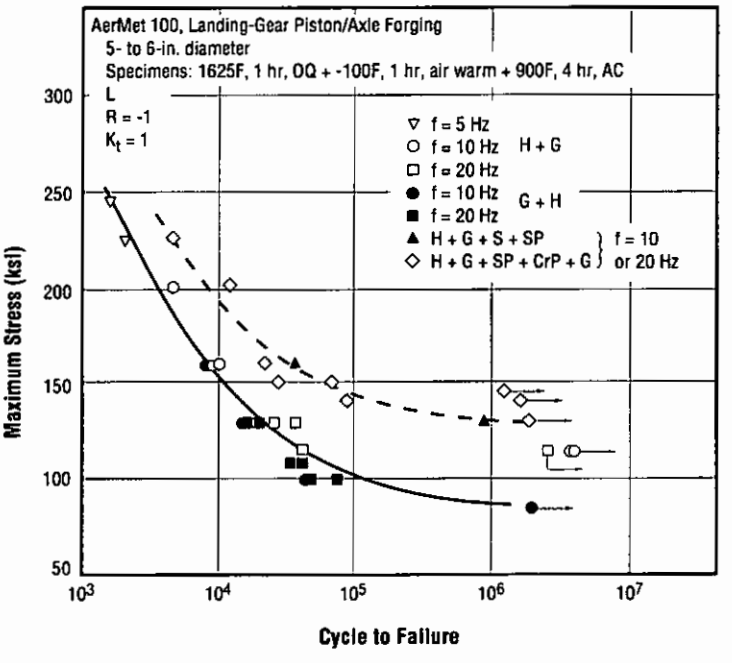

Fig. 3.5.1.1 Axial load fatigue data at R = - 1 for smooth specimens cut from a forging and tested with various surface conditions at different frequencies (Ref. 13)

Surface Condition Code:

H = Heat treated
G = Ground, 63 rms
S = Sand blasted
SP = Shot peened
(0.008 to 0.012 Almen Intensity)
CrP = Chrome plated
M = Machined, 125 rms

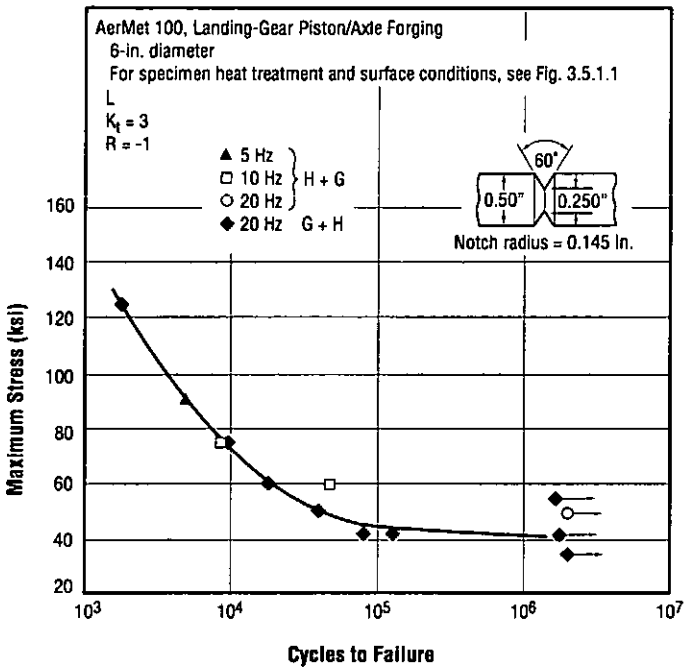

Fig. 3.5.1.2 Axial load fatigue data at R = - 1 and K_t = 3 for specimens cut from a forging and tested with various surface conditions at different frequencies (Ref. 13)

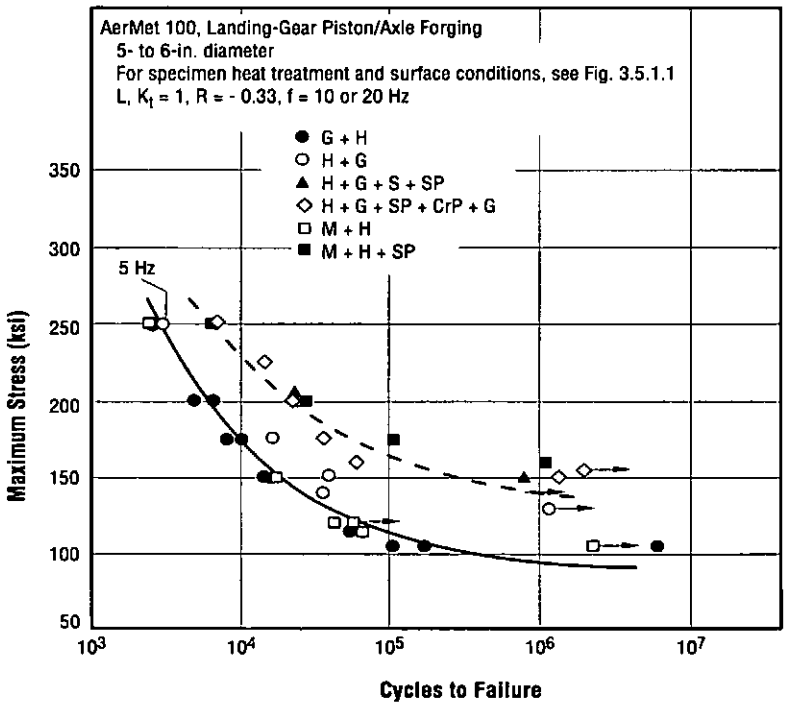

Figure 3.5.1.3 Axial load fatigue data at R = - 0.33 for smooth specimens cut from a forging and tested with various surface conditions at different frequencies (Ref. 13)

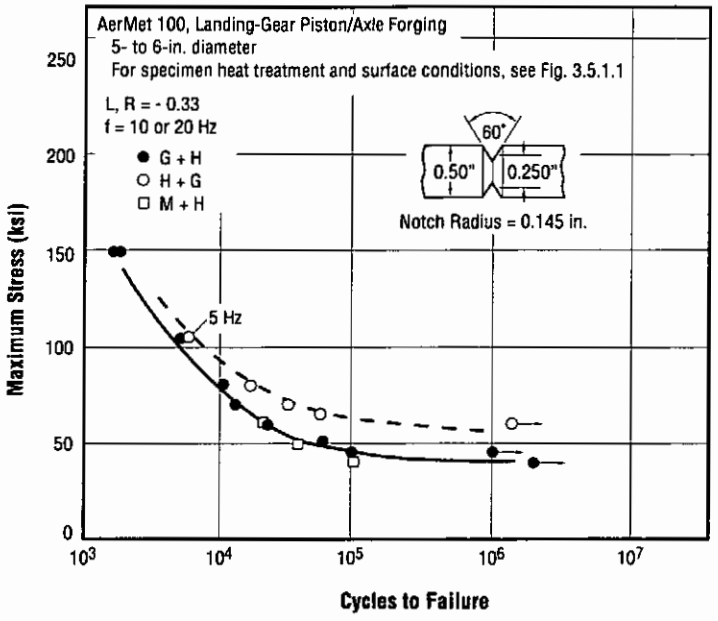

Figure 3.5.1.4 Axial load fatigue data at R = - 0.33 and K_t = 3 for specimens cut from a forging and tested with various surface conditions and at different frequencies (Ref. 13)

Table 3.5.1.5 Estimates of the fatigue strength at 10^6 cycles for axial loading of specimens from a landing-gear piston/axle forging

Alloy	AerMet 100										
Form	Landing-Gear Piston/Axle Forging										
Heat Treatment	See Fig. 3.5.1.1										
Sources	Figures 3.5.1.1 to 3.5.1.4 (Ref. 13)										
R Ratio	-1					- 0.33					
Stress Concentration, K_t	1			3		1				3	
Surface Condition[a]	G+H	H+G	SP	G+H	H+G	G+H	H+G	M+H	SP	G+H	H+G
Maximum Stress at 10^6 cycles (ksi)	75	120	140	50		110	125		170	60	50

[a] See Fig. 3.5.1.1 for surface conditions.

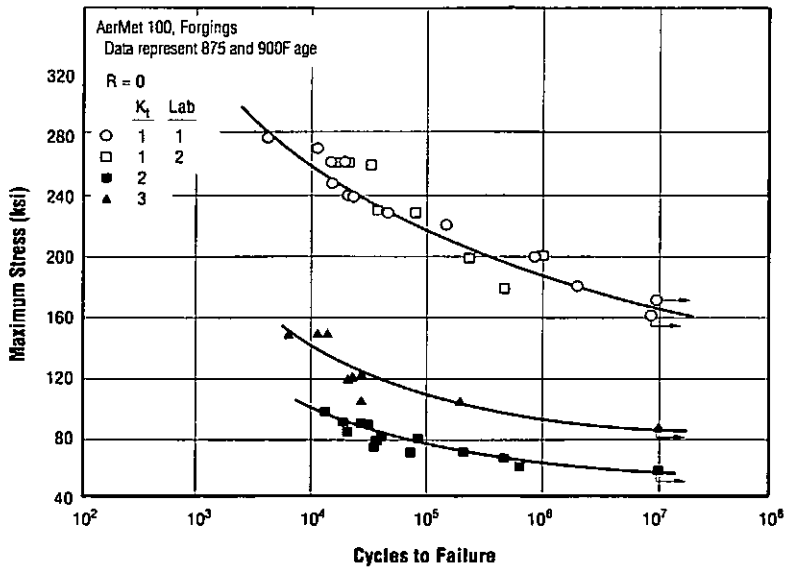

Fig. 3.5.1.6 Fatigue data for forgings tested at R = 0 using smooth and notch specimens of unspecified geometry (Refs. 2, 10)

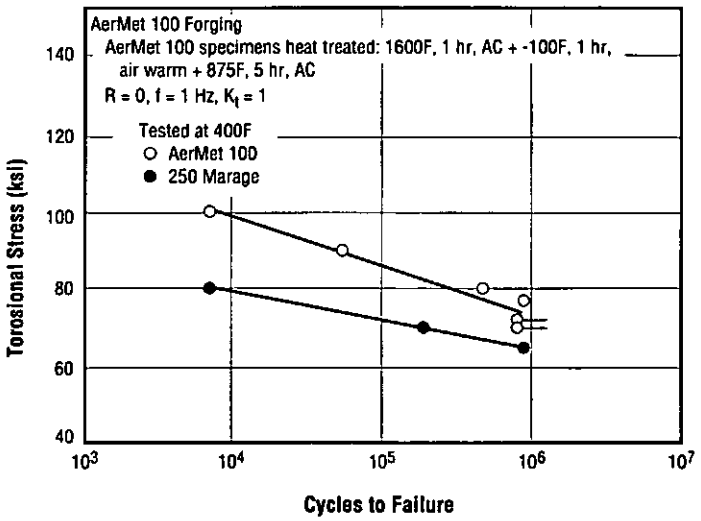

Figure 3.5.1.7 Torsional fatigue strength at 400F of AerMet 100 and 250 Grade Maraging steel (Ref. 9)

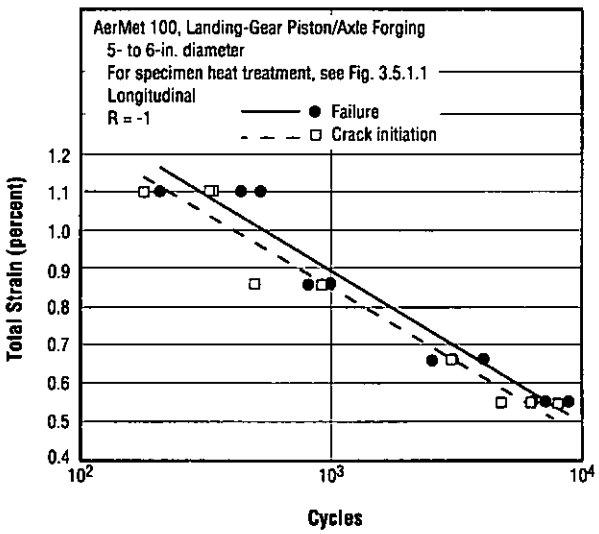

Figure 3.5.2.1 Low cycle fatigue data for crack initiation and failure for specimens cut from a forging (Ref. 13)

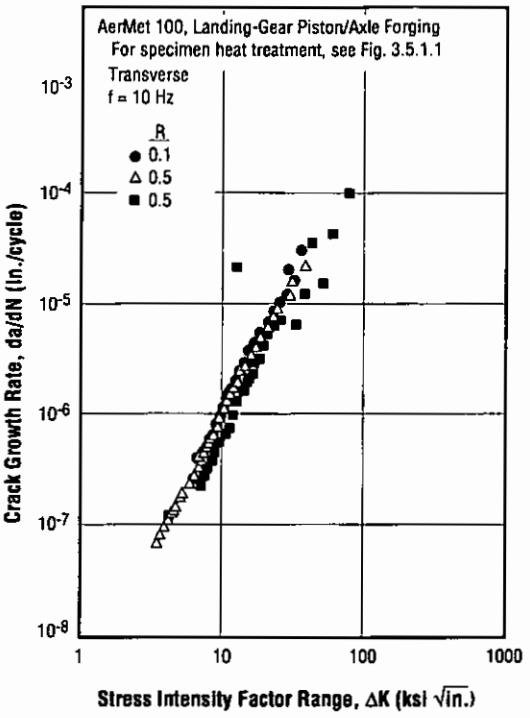

Fig. 3.5.3.1 Fatigue crack propagation rates in air at several R values for landing-gear piston/axle forging (Ref. 13)

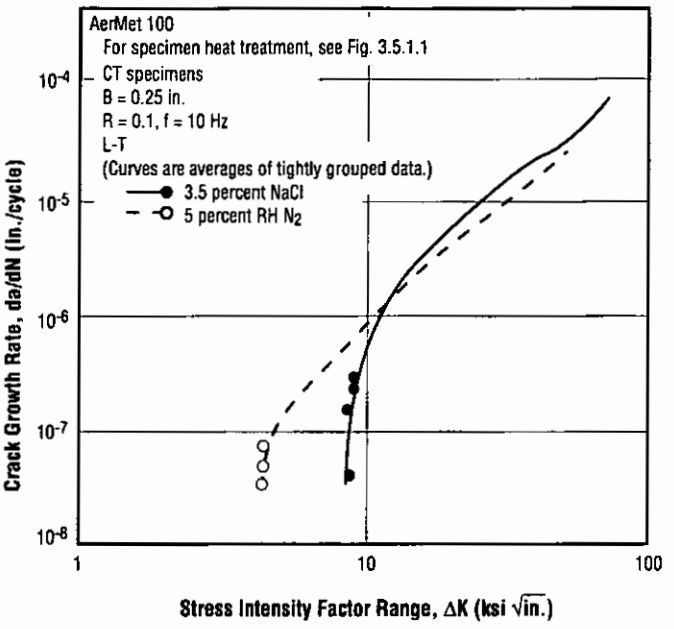

Fig. 3.5.3.2 Fatigue crack growth rates at R = 0.1 in 3.5 percent NaCl and in dry nitrogen for a forged slab (Ref. 7)

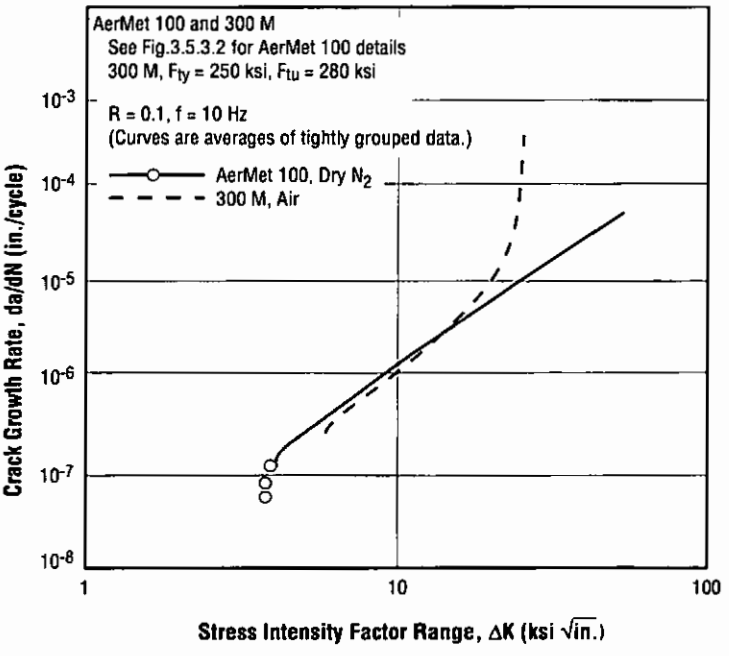

Fig. 3.5.3.3 Fatigue crack growth rates at R = 0.1 for AerMet 100 in dry nitrogen and 300 M in air (Ref. 7)

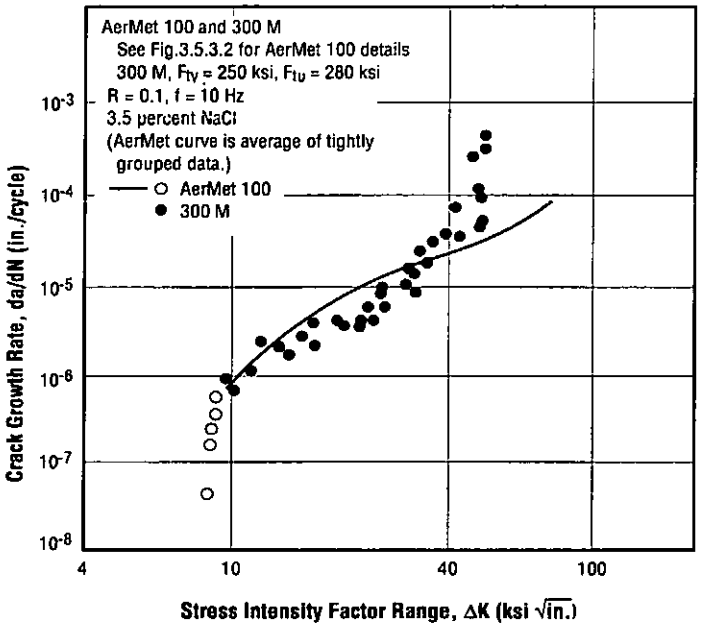

Fig. 3.5.3.4 Fatigue crack growth rates at R = 0.1 for AerMet 100 and 300 M in 3.5 percent NaCl (Ref. 7)

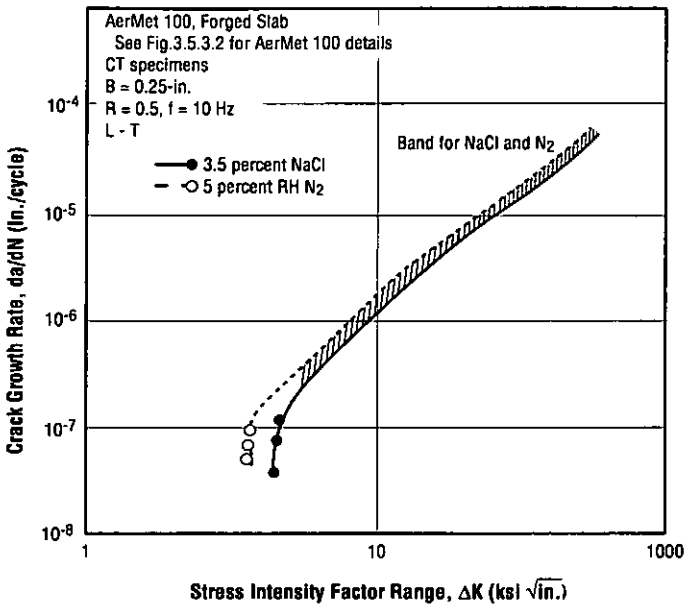

Fig. 3.5.3.5 Fatigue crack growth rates at R = 0.5 in 3.5 percent NaCl and in dry nitrogen for a forged slab (Ref. 7)

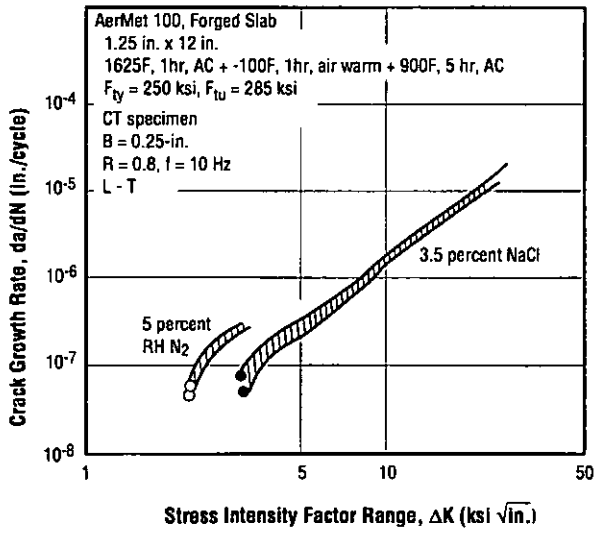

Fig. 3.5.3.6 Fatigue crack growth rates at R = 0.8 in 3.5 percent NaCl and in dry nitrogen for a forged slab (Ref. 6)

Table 3.6.2.1 Tension and compression moduli of elasticity determined for specimens aged at 875F which were cut from various size forgings representing seven heats (Ref. 2)

Alloy	AerMet 100	
Form	Forgings	
Condition	See Fig. 3.5.1.8	
Sizes		
Direction	Longitudinal[a]	
Modulus (10^3 ksi)	Tension	Compression
Mean	27.9	28.2
Standard Deviation	0.3	

[a] Sampling - 30 tests for each property.

Table 4.3.1.1 Preliminary results (duplicate tests) for tensile properties and Charpy V impact energies for GTA welds in plate (Refs. 2, 19)

Alloy	AerMet 100			
Form	60° V-groove GTA multiple-pass welds in 5/8-in. plate			
Condition[a]	A A+W+N+A+STA	B STA+W	C STA+W+SR	D STA+W+Age
F_{tu} (ksi)	281 280	262 260	260 260	268 266
F_{ty} (ksi)	253 252	181 183	176 186	230 233
Elongation, e (percent)	14 13	10 8	15 11	13 8
Reduction in Area, RA (percent)	60 59	16 23	56 25	30 28
Charpy V Impact Energy[b] (ft-lb)	22 27	-	25 24	20 21

[a] A - Anneal 1250F, 16 hr, AC; W - GTA weld; N - Normalize 1650F, 1 hr, AC; SR - Stress relief 200F, 5 hr, AC; STA - 1625F, 1 hr, AC + -100F, 1 hr, Air warm + 900F, AC.

[b] Specimens taken at weld center line.

References

1. Military Handbook 5G, "Metallic Materials and Elements for Aerospace Vehicle Structures", prepared by the U.S. Air Force, November 1994
2. Personal communication from P.M. Novotny, Carpenter Technology, to W. F. Brown Jr. March 29, 1995
3. Aerospace Material Specification, AMS 6478, Society of Automotive Engineers, May 1994.
4. Ruff, P.E.,"Mechanical Properties of AerMet 100 Alloy", *Carpenter Technology Report*, February 14, 1995.
5. Novotny, P. M., "An Aging Study of Carpenter AerMet 100 Alloy", 1992 Gilbert R.Spiech Symposium Proceedings, Fundmentals of Aging and Tempering in Martenistic and Banitic Steel Products, Iron and Steel Institute, Eds. G. Kraus and P.E. Repas, 1992. p.215
6. Wert. D.E., "Statistical Analysis of AerMet 100 Alloy", *Carpenter Steel*, Oct. 11, 1991.
7. Lee E. U., "Fatigue Crack Growth in AerMet 100 Steel", Naval Air Development Center, Report No. NASC-91111-60, Oct. 18, 1991.
8. Novotny, P. M., "Effect of Variations in Hardening and Aging Parameters on the Fracture Toughness and Tensile Properties of Carpenter AerMet 100 Alloy", *Carpenter Research and Technology*, 1991.
9. Novotny, P. M. and Dahl, J. M., "AerMet 100 Alloy for Aerospace Applications", Mechanical Working and Steel Processing Proceedings, 1990, p. 275.
10. Henderson, J. B. , Groot, H. and Ferrier, J.,"Thermal Physical Properties of an Iron Alloy", Report to Carpenter Technology, Purdue University, School of Mechanical Engineering, Report TPRL 1222, Nov. 1992.
11. Alloy Data, "AerMet 100 Alloy", *Carpenter Technology*, 1992
12. Kozol, J. and Neu, C.E., "Stress Corrosion Susceptibility of Ultra High Strength Steels for Naval Aircraft Applications", Report No. NAWCADWAR-92018-60, Naval Air Warfare Center, Jan. 10, 1992.
13. Personal Communication from R. Eybel, Dowty Aerospace, Ontario, Canada, April 1995.
14. Raghavan, A. and Machmeier, P.M., "Analytical Electron Microscopic Examination of Peak Hardening Phenomena in a Secondary Hardening High Strength Steel", Microstructure and Mechanical Properties of Aging Material, The Minerals, Metals and Materials Society, 1993
15. Aerospace Materials Specification, AMS 6532, Society of Automotive Engineers, June 1992
16. Novotny, P. M. and McCaffery, T.J., "An Advanced Alloy for Landing Gear and Aircraft Structural Applications - AerMet 100 Alloy", SAE Technical Paper 922040, 1992.
17. Dahl, J., "AerMet 100 - An Advanced Steel for the Aerospace Industry", *Advanced Materials Technology International*, 1991
18. Novotny, P.M. and Maguire, M. "Navy Fighter Demands Evolve into Tough Castings", *Foundry Management and Technology*, December 1993, p.33
19. Novotny, P.M., Nye, R.D., and Robino, C.V., "Fabricating Characteristics of Ultrahigh-Strength Steel", *Welding Journal*, Feb. 1995